chemosensors

Article

Molecular Understanding of the Surface-Enhanced Raman Spectroscopy Salivary Fingerprint in People after Sars-COV-2 Infection and in Vaccinated Subjects

Francesca Rodà [1,2], Alice Gualerzi [2,*], Silvia Picciolini [2], Luana Forleo [2], Valentina Mangolini [2,3], Roberta Mancuso [2], Simone Agostini [2], Rudy Alexander Rossetto [4], Paola Pierucci [5,6], Paolo Innocente Banfi [2] and Marzia Bedoni [2,*]

1 Clinical and Experimental Medicine PhD Program, University of Modena and Reggio Emilia, 41125 Modena, Italy; froda@dongnocchi.it
2 IRCCS Fondazione Don Carlo Gnocchi ONLUS, 20148 Milan, Italy; spicciolini@dongnocchi.it (S.P.); lforleo@dongnocchi.it (L.F.); vmangolini@dongnocchi.it (V.M.); rmancuso@dongnocchi.it (R.M.); sagostini@dongnocchi.it (S.A.); pabanfi@dongnocchi.it (P.I.B.)
3 Department Molecular and Translational Medicine (DMMT), University of Brescia, 25122 Brescia, Italy
4 Ordine dei Biologi della Lombardia, 20057 Assago, Italy; dott.rossetto@gmail.com
5 Cardiothoracic Department, Respiratory and Critical Care Unit, Bari Policlinic University Hospital, 70124 Bari, Italy; paola.pierucci@policlinico.ba.it
6 Section of Respiratory Diseases, Department of Basic Medical Science Neuroscience and Sense Organs, University of Bari 'Aldo Moro', 70121 Bari, Italy
* Correspondence: agualerzi@dongnocchi.it (A.G.); mbedoni@dongnocchi.it (M.B.); Tel.: +39-0240308874 (M.B.)

Abstract: The rapid spread of SARS-COV-2 and the millions of worldwide deaths and hospitalizations have prompted an urgent need for the development of screening tests capable of rapidly and accurately detecting the virus, even in asymptomatic people. The easy collection and the biomarker content of saliva, together with the label-free and informative power of surface-enhanced Raman spectroscopy (SERS) analysis have driven the creation of point-of-care platforms capable of identifying people with COVID-19. Indeed, different salivary fingerprints were observed between uninfected and infected people. Hence, we performed a retrospective analysis of SERS spectra from salivary samples of COVID-19-infected and -vaccinated subjects to understand if viral components and/or the immune response are implicated in spectral variations. The high sensitivity of the proposed SERS-based method highlighted the persistence of molecular alterations in saliva up to one month after the first positive swab, even when the subject tested negative for the rapid antigenic test. Nevertheless, no specific spectral patterns attributable to some viral proteins and immunoglobulins involved in COVID-19 infection and its progression were found, even if differences in peak intensity, presence, and position were observed in the salivary SERS fingerprint.

Keywords: saliva; Raman spectroscopy; COVID-19; spike protein

check for updates

Citation: Rodà, F.; Gualerzi, A.; Picciolini, S.; Forleo, L.; Mangolini, V.; Mancuso, R.; Agostini, S.; Rossetto, R.A.; Pierucci, P.; Banfi, P.I.; et al. Molecular Understanding of the Surface-Enhanced Raman Spectroscopy Salivary Fingerprint in People after Sars-COV-2 Infection and in Vaccinated Subjects. *Chemosensors* **2024**, *12*, 136. https://doi.org/10.3390/chemosensors12070136

Received: 28 May 2024
Revised: 29 June 2024
Accepted: 9 July 2024
Published: 11 July 2024

Copyright: © 2024 by the authors. Licensee MDPI, Basel, Switzerland. This article is an open access article distributed under the terms and conditions of the Creative Commons Attribution (CC BY) license (https://creativecommons.org/licenses/by/4.0/).

1. Introduction

The COVID-19 pandemic, caused by the Sars-COV-2 virus, became a worldwide health emergency that caused deaths and radical changes in our habits. Belonging to the coronavirus family, Sars-COV-2 displays an affinity towards the ACE-2 receptor, resulting in a principal involvement of the upper and lower airways. The coronas of spike proteins around the virus mediate the receptor binding through subunit 1, while subunit 2 is responsible for virus–host–cell membrane fusion [1]. Over these four years, this wild virus form has undergone spontaneous mutations, causing the appearance of five variants of concern responsible for increased transmission. It also has a variability of symptoms [2,3]. Its clinical manifestations range from fever, cough, sore throat, and muscle pain to pneumonia and death in the most severe cases. To slow down the spread of the virus and decrease

the mortality rate, anti-COVID-19 vaccines were developed. Based on mRNA technology, Comirnaty (BNT162b2) (Pfizer-BioNTech®) and Spikevax (Moderna®) vaccines were the ones mainly administered in Italy [4]. The induced immunological memory, through the production of anti-Sars-COV-2 spike protein antibodies, prevents the worsening of the disease and should reduce contagiousness [5]. Additionally, a variety of diagnostic methods for different contexts has been developed. RT-PCR molecular test and the rapid antigen immuno-based test are the two gold-standard techniques performed mainly using a nasopharyngeal swab. The presence of the virus is verified through the quantification of the genetic material and the detection of viral proteins, respectively. Although RT-PCR is a very sensitive technique, it is time-consuming and expensive, while the rapid antigen test allows fast screening at the expense of accuracy [6,7]. In this context, saliva has attracted interest as a specimen for COVID-19 diagnosis for the self because of its non-invasive and painless collection, and since it is a reservoir of a variety of molecules, diseases-related biomarkers, and viruses [8–10]. Sars-COV-2 can persist in saliva for up to about 20 days after the onset of symptoms, causing alterations in the lipid and inflammatory profile, T-cells, metabolites, and proteins [11–13]. Given the concordance of the results with the nasopharyngeal swab, saliva has been confirmed as a valid alternative and has been employed in some COVID-19 tests [14–16]. However, new diagnostic tools have been created to address some of the limitations of conventional platforms. Among them, surface-enhanced Raman spectroscopy (SERS) has emerged as a valuable analysis thanks to its high-sensitivity ability to detect the lowly concentrated molecules present in saliva. Indeed, the use of metallic substrates enhances the Raman effect, providing more accurate biomolecular information [17–21]. From 2020, about 20 papers have been published on this topic. Most studies involve the creation of SERS-based immunoassays for the detection of viruses by spike and/or nucleocapsid proteins or receptor-binding domain recognition, employing artificial or human saliva samples enriched with viral proteins or particles [22–26]. Although these methods can detect very low concentrations of viral components, they are expensive, variant-dependent (as they involve the use of antibodies), and do not fully mirror the real condition. Alternatively, the whole salivary spectrum can be considered a fingerprint of the individual's status of health, avoiding the use of reagents. The possible clinical application of a label-free SERS platform for COVID-19 diagnosis is supported by good levels of accuracy, precision, and specificity, also achieved using machine learning algorithms. Alterations of the salivary Raman spectrum mirror the modifications in saliva due to the infection. In most of the works, spectral variations are attributable to proteins, nucleic acids, and lipids. In our previous study, we were able to discriminate subjects positive for Sars-COV-2 from those with a past infection or uninfected with a diagnostic accuracy between 89% and 92% [27]. Indeed, a specific salivary Raman fingerprint was ascribable for each experimental group, with spectral variations related to O–O stretching, glucose/glycogen, C–N, and C–C protein stretching, tryptophan, phenylalanine, and secondary bands of amide III. Along the same line, Ember K. et al. found differences in the ranges of proteins, DNA, urea salt, and nitrate by comparing the spectra of the main saliva constituents [28]. Moreover, the involvement of methionine and tyrosine has been suggested due to variations in the intensity bands at 654, 720, 1320, 1443 cm^{-1}, 828, and 853 cm^{-1}, respectively, between positive and negative subjects [29]. However, no study has delved into the possible molecules behind these differences in the Raman spectra. Tentative assignations of the peaks were made based on the literature data and molecular alterations in the saliva after infection. Since Raman bands could derive from different molecules, the aim of this study was to better understand which molecules are involved in saliva spectra variance. Specifically, we studied the involvement of the Sars-COV-2 virus by investigating the potential implication of the spike and nucleocapsid proteins, and of the immune system. For this purpose, we performed a study on both COVID-19 subjects and healthy ones after the administration of the Comirnaty® vaccine.

2. Materials and Methods

2.1. Saliva and Serum Sample Collection

This study was approved by the Ethics Committee of IRCCS Fondazione Don Carlo Gnocchi ONLUS on 17 February 2021 and 20 May 2021. All participants gave written informed consent and filled out a brief questionnaire about smoking habits and ongoing pharmacological treatments. Eventual oral infections, recent dental surgeries, and pathologies of the respiratory system were recorded. The study involved 38 volunteers who were divided into two groups, following a different timeline in the saliva collection. The first group (Group 1), consisting of 17 people, collected saliva once a week for one month after the first positive nasopharyngeal test. The positivity of Sars-COV-2 was diagnosed by nasal rapid antigen test and hospitalisation was not needed. The second group (Group 2) consisted of 21 hospital co-workers. The saliva sampling was performed before starting the anti-COVID-19 vaccine cycle and 30 days after the second dose of the Pfizer vaccine (Comirnaty®). Stimulated saliva samples were self-collected using Salivette® (Sarstedt AG & CO, Numbrecht, Germany), processed following our previously optimised protocol, and stored at –20 °C until use [27]. Before all the analyses, saliva aliquots were thawed and vortexed to guarantee sample homogeneity. Serum samples for immunoglobulin quantification were collected from Group 2 30 days after the second dose using collection tubes with a gel separator (BD Vacutainer®SST™ II Advance tubes, Becton-Dickinson Biosciences, San Josè, CA, USA). Aliquots of serum samples were stored at −80 °C until use.

2.2. Preparation of Spike Protein Sample

The Sars-COV-2 spike protein (2019-nCoV Spike Protein S—Adipogen, Füllinsdorf, Switzerland) was reconstituted in sterile water, obtaining a final concentration of 10^{-6} M. Then, the stock solution was diluted in a Sars-COV-2 negative saliva sample to final concentrations of 10^{-7} and 10^{-9} M, based on literature data [30].

2.3. Surface-Enhanced Raman Spectroscopy Analysis

SERS spectra were collected using the Raman microscope Aramis (Horiba Jobin-Yvon, France) coupled with a laser source at 785 nm (150 mW power emission at source). The analysis of saliva was performed as previously described [27]. A saliva drop was dried at room temperature on a glass slide covered with commercial aluminium foil, and, for each subject, at least 15 spectra were collected in random points, given the reproducibility of the SERS spectra (Figure S1). The spectral regions of interest were 435–690 and 700–1600 cm^{-1}. The silicon spectrum was measured every day for Raman shift calibration to have accurate, reliable, and reproducible measurements. The same protocol was followed for the acquisition of the 15 spectra of spike solutions and saliva in which the protein was diluted. Compared to our previous work, the contribution of the aluminium substrate was not removed to minimise the manipulation of the spectra.

2.4. SERS Data Processing

The raw data of the saliva samples were subjected to post-processing using LabSpec6 (Horiba, France). Specifically, spikes and artefact spectra were removed, and a Savitsky–Golay smoothing filter of order 3 and a fifth-degree polynomial curve were applied. After alignment to the 1252 cm^{-1} band, spectra were extracted with a final resolution of 1.21 cm^{-1}/step, corresponding at 939 x-axis points. The resulting spectra were normalised by dividing each curve by the dataset norm using OriginLab2021b (OriginLab, version 2021, Northampton, MA, USA). Spectra of spike proteins underwent the same processing steps. The average of each saliva sample was used as input for the principal component analysis (PCA). For the comparative study among uninfected subjects and those with current and past infection, the first 7 principal components (PCs) were extracted and used for the creation of the classification model using linear discriminant analysis (LDA). An agglomerative hierarchical analysis was carried out on the 21 average spectra

of Group 2-timepoint 1. Statistical analysis was performed using one-way ANOVA for pair-wise comparisons, and the significance is indicated in the figures as * $p < 0.001$.

2.5. Enzyme-Linked Immunosorbent Assay (ELISA)

Cortisol and nucleocapsid protein were quantified using a commercial ELISA salivary test (Cortisol ELISA Kit-R&D Systems, Biotechne, Minneapolis, MN, USA; SARS-COV-2 nucleocapsid protein ELISA Kit—Arigo Biolaboratories, Zhubei City, Taiwan) according to the manufacturer's protocol. A cortisol assay was performed on Group 1 saliva samples ($n = 17$), whereas the nucleocapsid protein was quantified only in COVID-19-positive subjects ($n = 35$, as shown in Figure 1). Saliva samples were diluted 5-fold (cortisol) and 2-fold (nucleocapsid) to be within the standard curve, and the optical intensity was measured within 30 min at 450 nm with a Clariostar microplate reader (BMG Labtech, Ortenberg, Germany).

2.6. Salivary and Serum IgA Quantification

The IgA antibodies specific to the recombinant receptor-binding domain (S1-RBD) of the spike protein (Wuhan-Hu-1) were measured in saliva (2-fold diluted) and serum (500-fold diluted) using a commercial ELISA kit assay (RayBio, CliniSciences, Guidonia Monticello, Rome, Italy), according to the manufacturer's instruction, as previously described [31]. IgA antibody titres were expressed as U/mL (units/mL; cut-off: 21.4 U/mL).

2.7. Serum IgG Quantification

The IgG antibodies specific to the SARS-COV-2 receptor-binding domain (RBD) of the spike protein were measured in a serum by chemiluminescence immunoassay, CLIA, (Access Immunoassay Systems; Beckman Coulter, Brea, CA, USA) as recommended by the manufacturers. IgG antibody titres were expressed as AU/mL (arbitrary units/mL; cut-off: 10 AU/mL).

3. Results and Discussion

3.1. Longitudinal COVID-19 Fingerprint

To investigate whether the progression of the Sars-COV-2 infection resulted in changes in the SERS fingerprint of the saliva, 17 people were asked to collect saliva every week for one month after being diagnosed with COVID-19 (COVID19+; T1, T2, T3, T4). The SERS analysis was performed following our previously optimised protocol that allows us to obtain the salivary fingerprint in a fast and reproducible manner [27]. Each subject was considered separately for the spectral analysis, as each had a different timing of negativisation from COVID-19. Indeed, for some participants, the infection lasted about a week, while some subjects remained positive for the entire duration of the study. Compared to our previous work, the people included in this study were aged between 26 and 71 years and showed mild symptoms that required home-based therapy following the indications of the general medicine practitioner and were thus not hospitalised. Figure 1 summarises the demographic and clinical data of Group 1 subjects.

Number	17
Age, years	42.6 (15.9)
Gender, female	11
Smoker	0

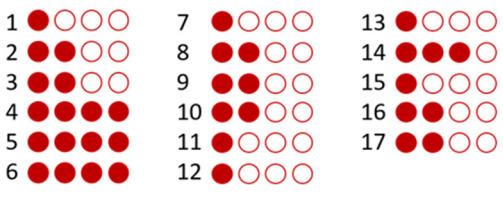


Figure 1. General information on COVID-19 subjects enrolled in this study. The standard deviation is reported in brackets. Dots indicate the saliva samples taken at time-points 1, 2, 3, 4. When the dot is filled, the subject is COVID-19 positive.

Figure 2 shows the overlaid mean spectra of the four time-points of subject 1, who tested positive for one week. The SERS spectra of samples of other subjects from Group 1 are present in the Supplemental Materials (Figure S2).

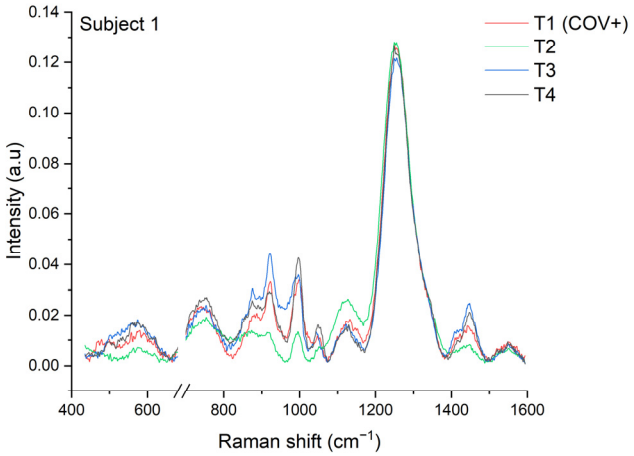


Figure 2. Overlapped average spectra of four time-points (T1, T2, T3, T4) of participant 1's saliva.

Comparing the four time-points, differences can be found mainly in the change in intensity and/or the presence and absence of specific peaks and bands. Some positive (#1T1, #8T1, #17T1, #12T1, #12T2) and negative (#1T3, #1T4, #8T2, #8T3, #17T2, #17T3, #1T4) saliva samples showed a band/shoulder at approximately 1420 cm^{-1} that can be related to the ring breathing modes of the DNA/RNA bases [32]. The peak at 852 cm^{-1}, attributable to glycogen, proline, or tyrosine, is also present indiscriminately in subjects with a current (COV+) and past (COV−) infection [33]. The same applies to the peak at 715 cm^{-1} related to phospholipids, which may be derived from the virion particle [27]. To better visualise possible spectral variations characteristic of disease progression, the spectrum at T4 was subtracted from T1. We selected these two time-points because, within a month, molecular changes are expected to occur independently of whether the subject is still positive or has become negative. The resulting subtraction spectra are displayed in Figure 3. Since all the subjects were positive at T1, the spectral area above the horizontal solid line (at zero intensity) is characteristic of the initial phase of the infection when the viral load is expected to be at maximum [34,35].

For three participants (#1/#2/#3), the subtraction spectrum is very noisy suggesting a similarity between the two time-points. Only subjects #4, #5, and #6 have three characteristic peaks at T1 (451, 620, and 990 cm^{-1}) while peaks at 715 and 1050 cm^{-1} well differentiate COV+ from COV− saliva of subjects #7 and #8. Nevertheless, the possible relationship of these peaks to the presence of the virus in saliva is contradicted by the subtraction spectrum of subject #9, which showed the opposite pattern. Lastly, the peaks at 920 (carbohydrates), 1000 (phenylalanine), and 1050 (tryptophan) cm^{-1} exhibited the greatest variation between T1 and T4 [27]; however, no discernible trend is evident. Already highlighted as one of the main differentiators in our previous work [27], the peak at 1050 can also be attributed to nitrates so we can speculate that its fluctuation may also depend on dietary habits [36].

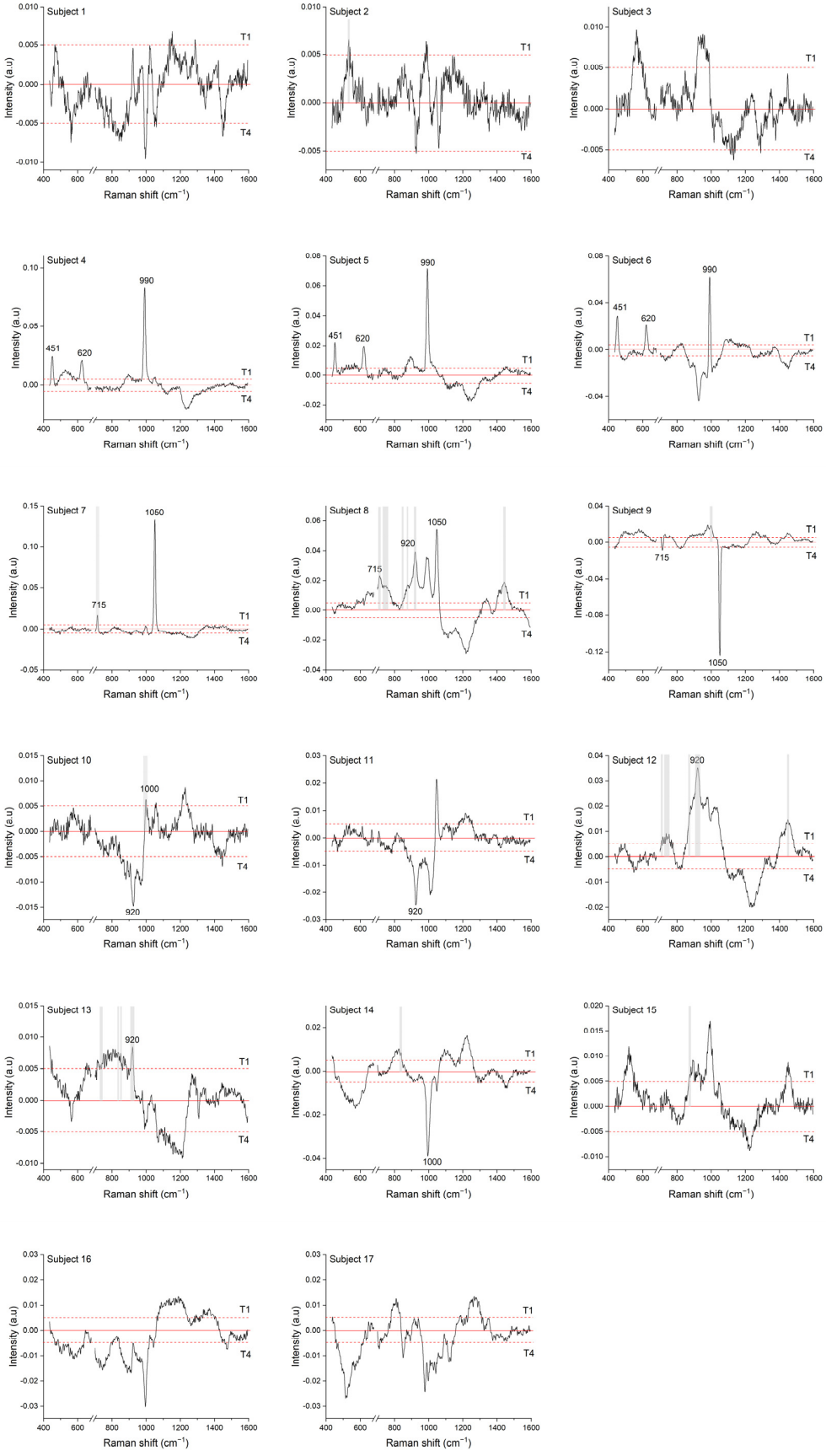


Figure 3. Subtraction spectra for each subject. The ± 0.005 ΔI interval was chosen as the lower limit for peak attribution.

3.2. Multivariate Analysis

In an effort to uncover potential differences not discernible from a simple comparison of spectra, multivariate statistical analysis was performed. After PCA, the obtained PC score distribution showed a minimal inter-group variation between the COV+ and COV− samples (Figure 4a), suggesting that the molecular alterations that occurred in saliva due to infection did not lead to major modifications in the SERS spectrum within a month. The inability to distinguish the COV+ from COV− samples, in contrast to our previous work [27], may be explained by the fact that in the present study, the COV− saliva samples were collected a short time after the negativization happened. Nevertheless, the loadings of the first three PCs, which account for about 75% of the variance, showed some variations at specific Raman shifts (Figure 4b). It has to be noted that despite the involvement of peaks at 451, 618, 712, 920, 990, 1049, 1418, and 1450 cm^{-1} in the differences between COV+ and COV− spectra, the areas under the curve of these spectral regions were not significantly different between the two groups (Figure S3, Supplementary Materials). Hence, to ascertain that our SERS approach is also suitable as a diagnostic platform for non-severe COVID-19 cases, a PCA-LDA was performed including the saliva samples of 36 healthy controls (CTRLs) used in the past work [27]. The first seven PCs were extracted and used for the classification model. As expected, the CTRLs significantly differ from the other two experimental groups, while the distribution of the canonical variable 1 highlighted no differences between COV+ and COV− (Figure 4c). This result is in agreement with our previous observation that negativized patients do maintain the biomolecular composition of saliva chemical alterations related to a previous infection by Sars-COV-2, even in mild cases of COVID-19. These variations make the SERS salivary fingerprint of subjects after COVID-19 significantly different from CTRL subjects (no previous infection by Sars-COV-2 registered) but partially overlapped with COV+. Disease severity, subjects' age, and sample size are possibly responsible for the differences in the present results, compared to previous data [27].

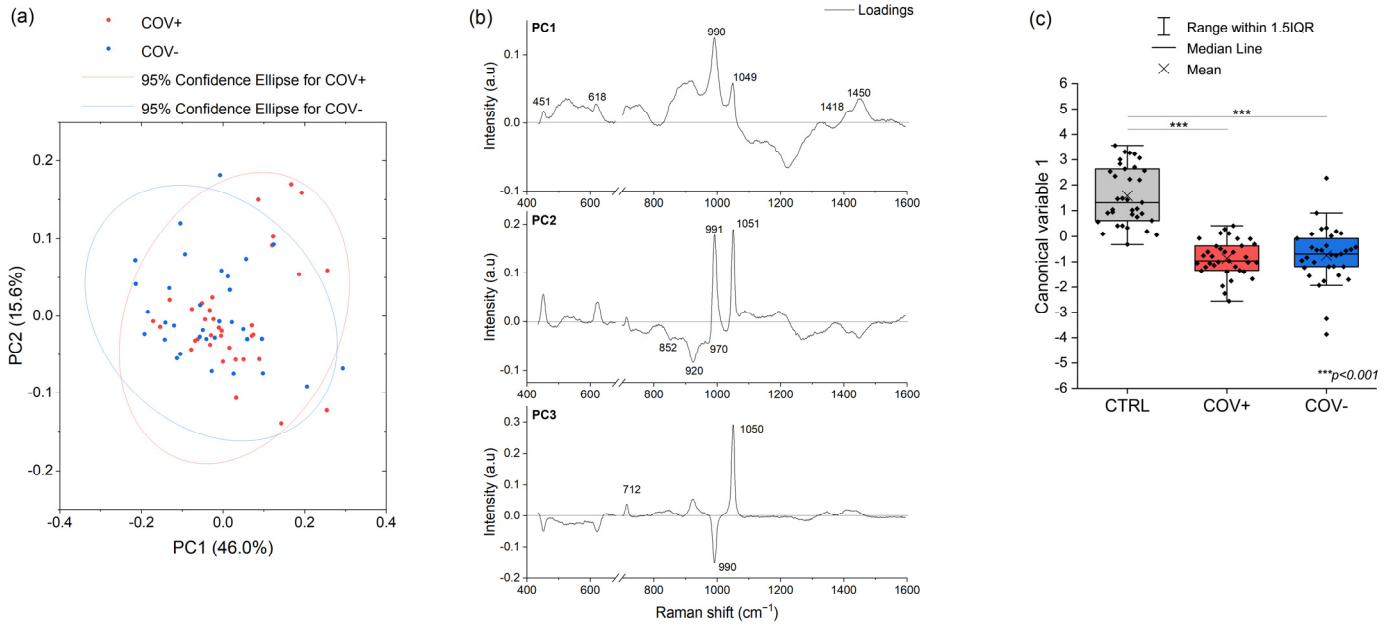


Figure 4. Results of the multivariate analysis. (**a**): PC1 and PC2 scores distribution. Each dot represents the average spectrum of each sample; (**b**): the loadings of the first three PCs; (**c**): the statistical analysis (one-way ANOVA test) on Canonical Variable 1, derived from the LDA of the CTRL, COV+, and COV− subjects.

3.3. Salivary Cortisol Quantification

Salivary cortisol was quantified to exclude any potential impact in the SERS spectrum since its level follows a circadian profile and is influenced by lifestyle, stress, and pathological conditions [37,38].The analysis was performed on all samples from Group 1 and samples at T1 from Group 2. Except for one specimen, all saliva samples had cortisol levels in the range of 0–20 ng/mL, which was in agreement with results reported in the literature [39,40]. Values are reported in Table S1 in the Supplementary Materials. Considering the Raman peaks characteristic of salivary cortisol [41], only the peak at 1450 cm^{-1} is present in our spectra, and no variations in its intensity or position were found. Therefore, we can determine that differences in salivary cortisol levels did not affect the obtained spectra in the considered analysis.

3.4. SERS Data Interpretation

3.4.1. Nucleocapsid Protein

To understand if the viral components are implicated in the discrimination of COVID-19 samples, we studied the potential contribution of the nucleocapsid protein. The COV+ saliva samples of Group 1 were tested for the presence of the Sars-COV-2 nucleocapsid protein. Unexpectedly, in most samples, the assay did not allow for nucleocapsid quantitation, as it was probably under the limit of detection of the techniques, whereas only two samples from the same subject (T1 and T2 of subject #7) contained the protein at a concentration of 15.2 and 15.6 ng/mL, respectively. Considering the Raman spectrum of the nucleocapsid protein [42], in #7T1 and #7T2, only the peak at 1050 cm^{-1} could refer to its presence, even though this peak is present indifferently in the COV+ and COV− spectra, with an intensity comparable to these two samples. In all the other COV+ specimens, the Sars-COV-2 nucleocapsid protein was not detectable by ELISA, although previously reported data showed that levels of up to 100 ng/mL were detected in saliva in the first ten days of infection using a single molecule array [43].

3.4.2. Spike Protein

The potential impact of the Sars-COV-2 spike protein in the SERS fingerprint was assessed through the SERS analysis of the protein itself in saliva. The averaged spectra of spike protein in saliva are presented in Figure 5a. The spectrum at 10^{-7} M is more informative in terms of peak presence and intensity. Interestingly, the shift of the peak from 920 cm^{-1} to 924 cm^{-1}, passing from 10^{-7} to the 10^{-9} M concentration, was observed. A red shift also involves the peak at 1046 that moves to 1053 cm^{-1} in the 10^{-9} M solution. These spectral areas were already identified as responsible for the inter-group variations. In contrast, only at the 10^{-9} M concentration is there the peak at 980 cm^{-1}, which has never previously been reported for the Sars-COV-2 spike protein solution. The observed concentration-dependent spectral variations are not surprising due to the expected alteration in ion–protein and protein–protein interactions in biological samples which are rich in both salts and proteins [44,45]. Although we cannot conclude if the observed shifts are related to spike-protein aggregates or to the interaction of the spike protein with other salivary components, we decided to consider for the subsequent analyses the spectra of saliva sample added with the 10^{-7} M protein that is expected to avoid the "crowding" effect.

To study the spectral contribution of the Sars-COV-2 protein in the saliva spectrum, we subtracted the spectrum of saliva from the spectrum of the same saliva sample added to the protein (10^{-7} M) (Figure 5b). The resulting subtraction spectrum is expected to show which peaks and bands are related to the spike protein in saliva. Spectral differences were considered significant for ± 0.005 ΔI. The Raman shift of the peaks related to the spike protein is listed in Table 1.

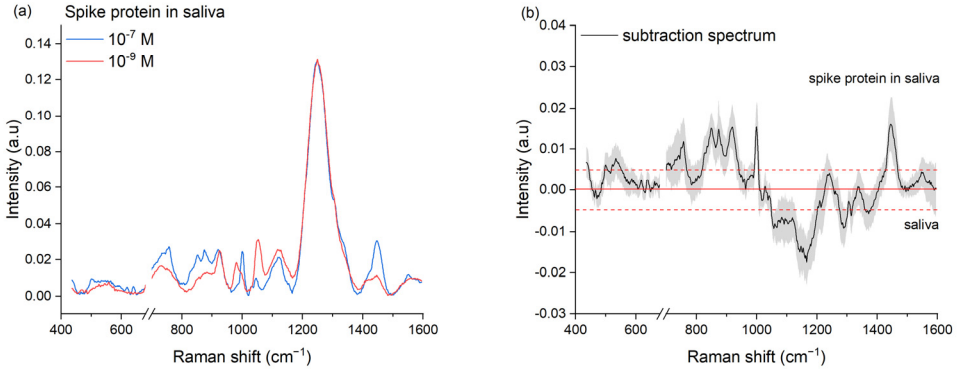


Figure 5. SERS analysis of spike protein added to saliva. (**a**) Overlapped SERS spectra of spike protein at two different concentrations; (**b**) subtraction spectrum of spike protein in saliva versus saliva. The grey area represents the propagation error.

Table 1. Peaks attributed to spike protein in saliva. Values refer to Raman shift (cm^{-1}).

500	702	738	835	999
521	707	741	849	1445
533	712	749	874	
538	728	758	884	
542	733	828	919	

Our data are in line with previous literature that identified 500, 542, 849, 874, 920, and 1445 cm^{-1} as the featured peaks of the Sars-COV-2 spike protein [42]. Thus, to demonstrate the contribution of the spike protein in COV+ saliva samples, we compared these values with the peaks observed in the subtraction spectra and referred to the T1 time-point that was expected to have a higher viral load. The comparison demonstrated the contribution of the Sars-COV-2 spike protein to the salivary fingerprint of some COV+ saliva samples at T1 (subjects #2, #7, #8, #12, #13, #14, #15). The grey bands in Figure 3 represent these common peaks and show that the spectral region with the greatest similarity is between 700 and 920 cm^{-1}. Additionally, since the 920 cm^{-1} peak was identified in the subtraction spectrum as belonging to the spike protein, and its position varies according to concentration, the Raman shift of this peak was evaluated in all saliva samples. Interestingly, a red shift was observed in samples from the same subject from T1 to T4 for samples #2, #11, #12, and #13 (Table 2), suggesting a decrease in spike protein concentration over time. Even the presence and/or the intensity of the peak at 920 cm^{-1} is not always visible in COV+ spectra, maybe due to the spike proteins' concentrations that are not detectable by SERS in such a complex specimen. Moreover, its correlation with Sars-COV-2 positive saliva is further strengthened by the fact that the spike protein is highly glycosylated [46]. On the other hand, albeit in a very small percentage, we observed the presence of these peaks in the T4 region of the subtraction spectrum. These observations may suggest the presence of the virus (or parts of the virus) one month after the first positive test, although, it has to be noted that a peak can result from the contribution of multiple molecules, and, thus, the spike protein, together with other molecules within saliva, might contribute to the same peak.

Table 2. Longitudinal variation of the Raman peak at around 920 cm^{-1}. (+) indicates a COV+ sample, while (-) indicates the peak absence.

Subject	T1	T2	T3	T4
4	918 (+)	919 (+)	919 (+)	924 (+)
5	918 (+)	920 (+)	920 (+)	921 (+)
6	920 (+)	923 (+)	-	-
9	920 (+)	920 (+)	924	924

3.5. Vaccination Fingerprint

To investigate the reasons for the observed overlap between COV+ and COV− saliva, the possible contribution of molecules associated with the immune response to Sars-COV-2 infection was hypothesised. Since immunoglobulins G (IgG) and A (IgA) are produced in response to the virus, we evaluated their possible involvement in the SERS spectrum. For this purpose, the saliva samples of 21 healthy hospital employees were analysed before starting the anti-COVID-19 vaccine cycle and one month after the second dose of the Pfizer vaccine to understand if the immune response could be detected in the SERS fingerprint of saliva. The timeline was selected because, at the second time-point (1 month after the second vaccine administration), the concentration of circulating antibodies produced against the virus is expected to reach their maximum. All the volunteers tested negative for Sars-COV-2 at both time-points, and only three subjects reported previous COVID-19 diagnoses. Table 3 summarises the demographic and clinical parameters.

Table 3. Clinical and demographic characteristics of the cohort of vaccinated volunteers. The standard deviation is reported in brackets.

Number	**21**
Age, years	42.8 (14.2)
Gender, female	13
Previous COVID-19	3

The average spectra of the two time-points (Tv0 and Tv1) are presented in Figure 6a. The two spectra presented the same pattern of peaks with very slight differences in terms of intensity. Thus, to identify if there are any intra-group relationships relating to spectral regions, a hierarchical cluster analysis of the T1 dataset was conducted. The resulting dendrogram highlighted two outliers and three clusters (Figure 6b). The spectra of these sub-groups underwent PCA to extract the PCs and study which peaks/bands were implicated in data separation. To verify if the spectral variations highlighted by the PC loadings could be related to the inter-individual fluctuation of immunoglobulins, PC1 scores were tested for correlation with the measured concentration of salivary IgA and with the serum concentration of IgA and IgG, but no correlation was assessed. Table S2 in the Supplementary Materials reported the level of the immunoglobulins quantified in saliva and serum, possibly due to the overlap between the Amide III region typically associated with IgA and IgG and the aluminium substrate interference.

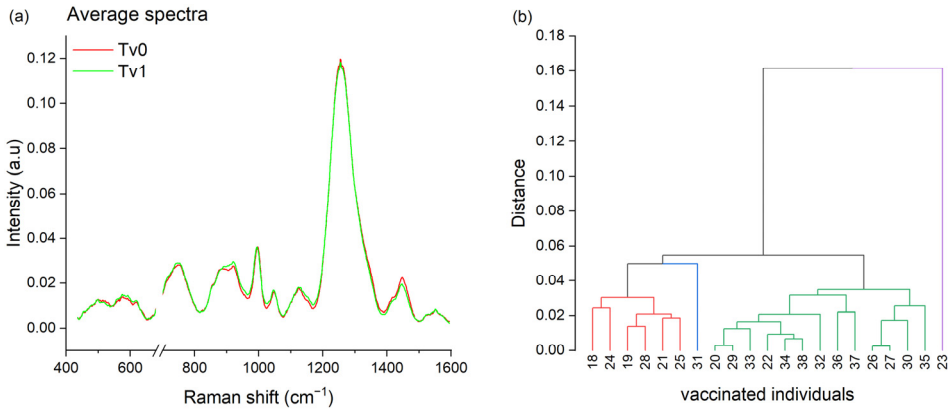


Figure 6. (**a**): Averaged SERS spectra of 21 saliva samples before (Tv0) and one month after the second dose of Pfizer vaccine (Tv1); (**b**) Hierarchical clustering dendrogram representing the unsupervised grouping of the SERS spectra at Tv1.

4. Conclusions

In the present work, we tried to decrypt the biomolecules involved in the modifications of the salivary SERS fingerprint of COV+ individuals by conducting a longitudinal study and taking into account some of the molecules that are expected to be detectable in saliva during Sars-COV-2 infection and after immunisation. Although COVID-19 is no longer a current emergency, the identification of the biomolecules involved in the biochemical alterations of saliva could possibly be used for the profiling of patients diagnosed with long-COVID disorders.

Our results demonstrate that SERS can identify a salivary biochemical fingerprint of people with a mild form of COVID-19 and that saliva composition is progressively modified after COVID-19 recovery. Indeed, after negativization, i.e., when the virus is no more detectable with standard nasopharyngeal rapid testing, saliva still retains biochemical features that resemble the biochemistry of saliva during COVID-19, even mild forms of the disease. However, compared to our previous work, the lack of differentiation between COV+ and COV− may be due to the different infection severity of the people involved in the study and the timing of saliva collection. Nonetheless, the modifications observed in saliva could not be associated either to Sars-COV-2 specific components (nucleocapside and spike protein) or to immunoglobulins that are expected to be released after the infection. Although this study was conducted on a limited cohort of subjects, because of the pandemic situation at the time of sample collection, our data support the ability of SERS applied to saliva to detect and monitor COVID-19 in a label-free and cost-effective manner. This technology holds promise as a point-of-care solution for the screening of other infectious respiratory diseases of significant global clinical importance, using a portable Raman device combined with clinician-friendly software.

Supplementary Materials: The following supporting information can be downloaded at: https://www.mdpi.com/article/10.3390/chemosensors12070136/s1, Figure S1. 15 spectra of Subject 1 at timepoint 1; Figure S2. Overlapping of the average spectra for the four timepoints for each subject; Figure S3. Comparison of areas under the curve between COV+ and COV− saliva samples; Table S1: Level of salivary cortisol (ng/mL) in the enrolled groups; Table S2. IgA and IgG levels in saliva and serum samples.

Author Contributions: Conceptualization, F.R., A.G., S.P. and M.B.; methodology, F.R., L.F., V.M., R.M. and S.A.; validation, A.G., R.M. and M.B.; formal analysis, F.R., A.G. and P.S; investigation, F.R., L.F. and S.A.; resources, F.R. and S.A.; data curation, R.M., P.I.B., P.P. and M.B.; writing—original draft preparation, F.R. and A.G.; writing—review and editing, S.P., L.F., V.M., R.M., S.A., P.I.B., P.P. and R.A.R.; visualisation, F.R., and S.P.; supervision, P.I.B. and M.B.; project administration, M.B.; funding acquisition, M.B. All authors have read and agreed to the published version of the manuscript.

Funding: This research was funded by the Italian Ministry of Health, Ricerca Corrente 2020–2022.

Institutional Review Board Statement: The study was conducted in accordance with the Declaration of Helsinki and approved by the Institutional Ethics Committee of FONDAZIONE DON GNOCCHI ONLUS (protocol code #6 and 30/2021/CE_FdG/FC/SA, 17 February 2021 and 20 May 2021).

Informed Consent Statement: Informed consent was obtained from all subjects involved in the study.

Data Availability Statement: All data generated or analysed during this study are included in this published article.

Acknowledgments: The authors would like to acknowledge Maria Langerame of Farmaacquisition s.r.l.

Conflicts of Interest: The authors declare no conflicts of interest.

References

1. Huang, Y.; Yang, C.; Xu, X.; Xu, W.; Liu, S. Structural and Functional Properties of SARS-CoV-2 Spike Protein: Potential Antivirus Drug Development for COVID-19. *Acta Pharmacol. Sin.* **2020**, *41*, 1141–1149. [CrossRef] [PubMed]
2. Magazine, N.; Zhang, T.; Wu, Y.; McGee, M.C.; Veggiani, G.; Huang, W. Mutations and Evolution of the SARS-CoV-2 Spike Protein. *Viruses* **2022**, *14*, 640. [CrossRef] [PubMed]

3. SARS-CoV-2 Variants of Concern as of 1 March 2024. Available online: https://www.ecdc.europa.eu/en/covid-19/variants-concern (accessed on 12 March 2024).
4. COVID-19 Medicines | European Medicines Agency. Available online: https://www.ema.europa.eu/en/human-regulatory-overview/public-health-threats/coronavirus-disease-covid-19/covid-19-medicines (accessed on 12 March 2024).
5. Rahman, M.M.; Masum, M.H.U.; Wajed, S.; Talukder, A. A Comprehensive Review on COVID-19 Vaccines: Development, Effectiveness, Adverse Effects, Distribution and Challenges. *Virusdisease* **2022**, *33*, 1–22. [CrossRef] [PubMed]
6. Afzal, A. Molecular Diagnostic Technologies for COVID-19: Limitations and Challenges. *J. Adv. Res.* **2020**, *26*, 149–159. [CrossRef] [PubMed]
7. Pérez-López, B.; Mir, M. Commercialized Diagnostic Technologies to Combat SARS-CoV2: Advantages and Disadvantages. *Talanta* **2021**, *225*, 121898. [CrossRef] [PubMed]
8. Khurshid, Z.; Zafar, M.; Khan, E.; Mali, M.; Latif, M. Human Saliva Can Be a Diagnostic Tool for Zika Virus Detection. *J. Infect. Public Health* **2019**, *12*, 601–604. [CrossRef] [PubMed]
9. Zhang, C.-Z.; Cheng, X.-Q.; Li, J.-Y.; Zhang, P.; Yi, P.; Xu, X.; Zhou, X.-D. Saliva in the Diagnosis of Diseases. *Int. J. Oral Sci.* **2016**, *8*, 133–137. [CrossRef] [PubMed]
10. Chojnowska, S.; Ptaszyńska-Sarosiek, I.; Kępka, A.; Knaś, M.; Waszkiewicz, N. Salivary Biomarkers of Stress, Anxiety and Depression. *J. Clin. Med.* **2021**, *10*, 517. [CrossRef] [PubMed]
11. Saheb Sharif-Askari, N.; Soares, N.C.; Mohamed, H.A.; Saheb Sharif-Askari, F.; Alsayed, H.A.H.; Al-Hroub, H.; Salameh, L.; Osman, R.S.; Mahboub, B.; Hamid, Q.; et al. Saliva Metabolomic Profile of COVID-19 Patients Associates with Disease Severity. *Metabolomics* **2022**, *18*, 81. [CrossRef]
12. Muñoz-Prieto, A.; Rubić, I.; Gonzalez-Sanchez, J.C.; Kuleš, J.; Martínez-Subiela, S.; Cerón, J.J.; Bernal, E.; Torres-Cantero, A.; Vicente-Romero, M.R.; Mrljak, V.; et al. Saliva Changes in Composition Associated to COVID-19: A Preliminary Study. *Sci. Rep.* **2022**, *12*, 10879. [CrossRef]
13. Bernardo, R.A.; Roque, J.V.; de Oliveira Júnior, C.I.; Lima, N.M.; Machado, L.S.; Duarte, G.R.M.; Costa, N.L.; Sorgi, C.A.; Soares, F.F.L.; Vaz, B.G.; et al. Exploring Salivary Lipid Profile Changes in COVID-19 Patients: Insights from Mass Spectrometry Analysis. *Talanta* **2024**, *269*, 125522. [CrossRef] [PubMed]
14. Sapkota, D.; Søland, T.M.; Galtung, H.K.; Sand, L.P.; Giannecchini, S.; To, K.K.W.; Mendes-Correa, M.C.; Giglio, D.; Hasséus, B.; Braz-Silva, P.H. COVID-19 Salivary Signature: Diagnostic and Research Opportunities. *J. Clin. Pathol.* **2020**, *74*, 344–349. [CrossRef] [PubMed]
15. Azzi, L.; Maurino, V.; Baj, A.; Dani, M.; d'Aiuto, A.; Fasano, M.; Lualdi, M.; Sessa, F.; Alberio, T. Diagnostic Salivary Tests for SARS-CoV-2. *J. Dent. Res.* **2021**, *100*, 115–123. [CrossRef] [PubMed]
16. Tan, S.H.; Allicock, O.; Armstrong-Hough, M.; Wyllie, A.L. Saliva as a Gold-Standard Sample for SARS-CoV-2 Detection. *Lancet Respir. Med.* **2021**, *9*, 562–564. [CrossRef] [PubMed]
17. Carlomagno, C.; Gualerzi, A.; Picciolini, S.; Rodà, F.; Banfi, P.I.; Lax, A.; Bedoni, M. Characterization of the COPD Salivary Fingerprint through Surface Enhanced Raman Spectroscopy: A Pilot Study. *Diagnostics* **2021**, *11*, 508. [CrossRef] [PubMed]
18. Carlomagno, C.; Bertazioli, D.; Gualerzi, A.; Picciolini, S.; Andrico, M.; Rodà, F.; Meloni, M.; Banfi, P.I.; Verde, F.; Ticozzi, N.; et al. Identification of the Raman Salivary Fingerprint of Parkinson's Disease through the Spectroscopic—Computational Combinatory Approach. *Front. Neurosci.* **2021**, *15*, 704963. [CrossRef] [PubMed]
19. Hardy, M.; Kelleher, L.; de Carvalho Gomes, P.; Buchan, E.; Chu, H.O.M.; Goldberg Oppenheimer, P. Methods in Raman Spectroscopy for Saliva Studies—A Review. *Appl. Spectrosc. Rev.* **2022**, *57*, 177–233. [CrossRef]
20. Chisanga, M.; Muhamadali, H.; Ellis, D.I.; Goodacre, R. Enhancing Disease Diagnosis: Biomedical Applications of Surface-Enhanced Raman Scattering. *Appl. Sci.* **2019**, *9*, 1163. [CrossRef]
21. Buchan, E.; Hardy, M.; Gomes, P.d.C.; Kelleher, L.; Chu, H.O.M.; Oppenheimer, P.G. Emerging Raman Spectroscopy and Saliva-Based Diagnostics: From Challenges to Applications. *Appl. Spectrosc. Rev.* **2022**, *59*, 277–314. [CrossRef]
22. Zhang, M.; Li, X.; Pan, J.; Zhang, Y.; Zhang, L.; Wang, C.; Yan, X.; Liu, X.; Lu, G. Ultrasensitive Detection of SARS-CoV-2 Spike Protein in Untreated Saliva Using SERS-Based Biosensor. *Biosens. Bioelectron.* **2021**, *190*, 113421. [CrossRef]
23. Tuckmantel Bido, A.; Brolo, A.G. Digital SERS Protocol Using Au Nanoparticle-Based Extrinsic Raman Labels for the Determination of SARS-CoV-2 Spike Protein in Saliva Samples. *ACS Appl. Nano Mater.* **2023**, *6*, 15426–15436. [CrossRef]
24. Mohammadi, M.; Antoine, D.; Vitt, M.; Dickie, J.M.; Sultana Jyoti, S.; Wall, J.G.; Johnson, P.A.; Wawrousek, K.E. A Fast, Ultrasensitive SERS Immunoassay to Detect SARS-CoV-2 in Saliva. *Anal. Chim. Acta* **2022**, *1229*, 340290. [CrossRef] [PubMed]
25. Lai, S.; Liu, Y.; Fang, S.; Wu, Q.; Fan, M.; Lin, D.; Lin, J.; Feng, S. Ultrasensitive Detection of SARS-CoV-2 Antigen Using Surface-Enhanced Raman Spectroscopy-Based Lateral Flow Immunosensor. *J. Biophotonics* **2023**, *16*, e202300004. [CrossRef] [PubMed]
26. Dong, Y.; Yuan, X.; Zhuang, K.; Li, Y.; Luo, X. Simultaneous and Sensitive Detection of SARS-CoV-2 Proteins Spike and Nucleocapsid Based on Long-Range SERS Biosensor. *Anal. Chim. Acta* **2024**, *1287*, 342070. [CrossRef] [PubMed]
27. Carlomagno, C.; Bertazioli, D.; Gualerzi, A.; Picciolini, S.; Banfi, P.I.; Lax, A.; Messina, E.; Navarro, J.; Bianchi, L.; Caronni, A.; et al. COVID-19 Salivary Raman Fingerprint: Innovative Approach for the Detection of Current and Past SARS-CoV-2 Infections. *Sci. Rep.* **2021**, *11*, 4943. [CrossRef] [PubMed]

28. Ember, K.; Daoust, F.; Mahfoud, M.; Dallaire, F.; Ahmad, E.Z.; Tran, T.; Plante, A.; Diop, M.-K.; Nguyen, T.; St-Georges-Robillard, A.; et al. Saliva-Based Detection of COVID-19 Infection in a Real-World Setting Using Reagent-Free Raman Spectroscopy and Machine Learning. *J. Biomed. Opt.* **2022**, *27*, 025002. [CrossRef] [PubMed]
29. Berus, S.M.; Nowicka, A.B.; Wieruszewska, J.; Niciński, K.; Kowalska, A.A.; Szymborski, T.R.; Dróżdż, I.; Borowiec, M.; Waluk, J.; Kamińska, A. SERS Signature of SARS-CoV-2 in Saliva and Nasopharyngeal Swabs: Towards Perspective COVID-19 Point-of-Care Diagnostics. *Int. J. Mol. Sci.* **2023**, *24*, 9706. [CrossRef]
30. Yeh, Y.-J.; Le, T.-N.; Hsiao, W.W.-W.; Tung, K.-L.; Ostrikov, K.; Chiang, W.-H. Plasmonic Nanostructure-Enhanced Raman Scattering for Detection of SARS-CoV-2 Nucleocapsid Protein and Spike Protein Variants. *Anal. Chim. Acta* **2023**, *1239*, 340651. [CrossRef] [PubMed]
31. Mancuso, R.; Agostini, S.; Citterio, L.A.; Chiarini, D.; Santangelo, M.A.; Clerici, M. Systemic and Mucosal Humoral Immune Response Induced by Three Doses of the BNT162b2 SARS-CoV-2 mRNA Vaccines. *Vaccines* **2022**, *10*, 1649. [CrossRef]
32. Movasaghi, Z.; Rehman, S.; Rehman, I.U. Raman Spectroscopy of Biological Tissues. *Appl. Spectrosc. Rev.* **2007**, *42*, 493–541. [CrossRef]
33. Szymborski, T.R.; Berus, S.M.; Nowicka, A.B.; Słowiński, G.; Kamińska, A. Machine Learning for COVID-19 Determination Using Surface-Enhanced Raman Spectroscopy. *Biomedicines* **2024**, *12*, 167. [CrossRef] [PubMed]
34. Zhu, J.; Guo, J.; Xu, Y.; Chen, X. Viral Dynamics of SARS-CoV-2 in Saliva from Infected Patients. *J. Infect.* **2020**, *81*, e48–e50. [CrossRef] [PubMed]
35. To, K.K.-W.; Tsang, O.T.-Y.; Leung, W.-S.; Tam, A.R.; Wu, T.-C.; Lung, D.C.; Yip, C.C.-Y.; Cai, J.-P.; Chan, J.M.-C.; Chik, T.S.-H.; et al. Temporal Profiles of Viral Load in Posterior Oropharyngeal Saliva Samples and Serum Antibody Responses during Infection by SARS-CoV-2: An Observational Cohort Study. *Lancet Infect. Dis.* **2020**, *20*, 565–574. [CrossRef] [PubMed]
36. Pannala, A.S.; Mani, A.R.; Spencer, J.P.E.; Skinner, V.; Bruckdorfer, K.R.; Moore, K.P.; Rice-Evans, C.A. The Effect of Dietary Nitrate on Salivary, Plasma, and Urinary Nitrate Metabolism in Humans. *Free Radic. Biol. Med.* **2003**, *34*, 576–584. [CrossRef] [PubMed]
37. Hansen, A.M.; Garde, A.H.; Persson, R. Sources of Biological and Methodological Variation in Salivary Cortisol and Their Impact on Measurement among Healthy Adults: A Review. *Scand. J. Clin. Lab. Investig.* **2008**, *68*, 448–458. [CrossRef] [PubMed]
38. Nater, U.M.; Hoppmann, C.A.; Scott, S.B. Diurnal Profiles of Salivary Cortisol and Alpha-Amylase Change across the Adult Lifespan: Evidence from Repeated Daily Life Assessments. *Psychoneuroendocrinology* **2013**, *38*, 3167–3171. [CrossRef] [PubMed]
39. Umeda, T.; Hiramatsu, R.; Iwaoka, T.; Shimada, T.; Miura, F.; Sato, T. Use of Saliva for Monitoring Unbound Free Cortisol Levels in Serum. *Clin. Chim. Acta* **1981**, *110*, 245–253. [CrossRef] [PubMed]
40. Heaney, J.L.J.; Phillips, A.C.; Carroll, D. Aging, Health Behaviors, and the Diurnal Rhythm and Awakening Response of Salivary Cortisol. *Exp. Aging Res.* **2012**, *38*, 295–314. [CrossRef]
41. Moore, T.J.; Sharma, B. Direct Surface Enhanced Raman Spectroscopic Detection of Cortisol at Physiological Concentrations. *Anal. Chem.* **2020**, *92*, 2052–2057. [CrossRef]
42. Sanchez, J.E.; Jaramillo, S.A.; Settles, E.; Salazar, J.J.V.; Lehr, A.; Gonzalez, J.; Aranda, C.R.; Navarro-Contreras, H.R.; Raniere, M.O.; Harvey, M.; et al. Detection of SARS-CoV-2 and Its S and N Proteins Using Surface Enhanced Raman Spectroscopy. *RSC Adv.* **2021**, *11*, 25788–25794. [CrossRef]
43. Shan, D.; Johnson, J.M.; Fernandes, S.C.; Suib, H.; Hwang, S.; Wuelfing, D.; Mendes, M.; Holdridge, M.; Burke, E.M.; Beauregard, K.; et al. N-Protein Presents Early in Blood, Dried Blood and Saliva during Asymptomatic and Symptomatic SARS-CoV-2 Infection. *Nat. Commun.* **2021**, *12*, 1931. [CrossRef] [PubMed]
44. Batoulis, H.; Schmidt, T.H.; Weber, P.; Schloetel, J.-G.; Kandt, C.; Lang, T. Concentration Dependent Ion-Protein Interaction Patterns Underlying Protein Oligomerization Behaviours. *Sci. Rep.* **2016**, *6*, 24131. [CrossRef] [PubMed]
45. Quevedo, M.; Karbstein, H.P.; Emin, M.A. Concentration-Dependent Changes in the Reaction Behavior of Whey Proteins: Diffusion-Controlled or Transition State-Controlled Reactions? *Food Hydrocoll.* **2021**, *118*, 106745. [CrossRef]
46. Yao, H.; Song, Y.; Chen, Y.; Wu, N.; Xu, J.; Sun, C.; Zhang, J.; Weng, T.; Zhang, Z.; Wu, Z.; et al. Molecular Architecture of the SARS-CoV-2 Virus. *Cell* **2020**, *183*, 730–738.e13. [CrossRef] [PubMed]

Disclaimer/Publisher's Note: The statements, opinions and data contained in all publications are solely those of the individual author(s) and contributor(s) and not of MDPI and/or the editor(s). MDPI and/or the editor(s) disclaim responsibility for any injury to people or property resulting from any ideas, methods, instructions or products referred to in the content.